

# Longitudinal Modeling of a Road Vehicle: 4-Wheel Traction

Calequela J. T. Manuel <sup>a,1,\*</sup>, Max M. D. Santos <sup>b,2</sup>, Giane G. Lenzi <sup>b,3</sup>, Angelo M. Tusset <sup>b,4</sup>

<sup>a</sup> Ph.D. student in Industrial Engineering, Federal University of Technology - Paraná, Ponta Grossa, PR, Brazil

<sup>b</sup> Department of Electronic Engineering, Federal University of Technology - Paraná, Ponta Grossa, PR, Brazil

<sup>1</sup> [calequelamanuel@alunos.utfpr.edu.br](mailto:calequelamanuel@alunos.utfpr.edu.br); <sup>2</sup> [maxsantos@utfpr.edu.br](mailto:maxsantos@utfpr.edu.br); <sup>3</sup> [gianeg@utfpr.edu.br](mailto:gianeg@utfpr.edu.br); <sup>4</sup> [tusset@utfpr.edu.br](mailto:tusset@utfpr.edu.br)

\* Corresponding Author

## ARTICLE INFO

## ABSTRACT

### Article history

Received April 27, 2022

Revised May 25, 2022

Accepted June 12, 2022

### Keywords

Computational modeling;

4-Wheel traction;

Longitudinal dynamics;

Calibration parameters;

Vehicular system;

Engine performance

This paper presents the longitudinal modeling of a 4-wheel traction vehicle represented in a block diagram using Matlab®/Simulink® software. The proposed modeling is suitable to be implemented in automatic parallel, oblique, or perpendicular parking systems considering speed cases between 5 km/h and 30 km/h. For the computational simulations, it was considered that the vehicle starts at rest and goes up a referenced or determined slope in degrees (°), with a sufficient rear reaction force to allow the vehicle to move until the engine produces sufficient torque. For the model of the tire variant, the magic formula (characterized by the sum of five vectors about an axis) was used. Three input signals were considered, slope, wind, and accelerator variation were considered in numerical simulations. The output signals are rear and normal front forces, vehicle speed, angular velocity, and engine acceleration. The longitudinal modeling proposed allows for easily reproducing the results and assigning new parameters to validate a Project, contributing positively both to the automotive industries and in innovation-based scientific research.

This is an open-access article under the [CC-BY-SA](https://creativecommons.org/licenses/by-sa/4.0/) license.



## 1. Introduction

There are different ways to determine the modeling parameters of a vehicle with 4-wheels [1-2], from its mathematical and computational modeling to being validated in a prototype or real vehicle [3], which can be standardized based on the dynamics and kinematics [4, 5] of the road vehicle. The main problem is the complexity of controlling the longitudinal movements (forward and/or backward) when the vehicle is in an inclined position and in operational mode. For this solution, a proper study is needed to define the specific parameters that directly influence the longitudinal modeling of a 4-wheel traction vehicle.

This paper aims to develop a mathematical model (represented in a computational way) that describes the kinematic and dynamic [6] model influenced by the position or movement longitudinal of the vehicle with 4-wheel drive in order to be used in real-time simulations to test and validate strategies of control [7-8]. In this introductory step, the vehicle model with a 4-wheel drive is presented through the Matlab®/Simulink® software, specifically, the Simulink® application [9], aiming at the application of this model in a parallel automatic parking system [10, 11, 12]. In order to be successful in this application, it is necessary to test and validate the vehicle model with the 4-wheel drive since it provides better accuracy and precision in the control strategy [13-15].

The papers with themes related to the proposed theme cited throughout this research present implicit diagrams for validation of the longitudinal modeling of a vehicle, i.e., they present only one diagram with input, transfer function, and output, and then show results:

However, the great differential of this paper in relation to the others cited throughout this research is due to the fact that it presents in a clear way the longitudinal modeling of the 4-wheeled vehicle through the sub-diagram (Fig. 1) with all elements used to test and validate the longitudinal modeling and is described the function of each block (Table 1) of the sub-diagram; allowing the reader an easy reproduction with the desired parameters to validate their project in the industry or for academic purposes.

As an innovation, this paper highlights/shows the proper control of the 4-wheeled vehicle operation from longitudinal modeling based mainly on the engine angular velocity range, recommended for performing automatic parking maneuvers with speeds of (5-30km) even considering inclination during vehicle displacement, without defining or integrating any auxiliary controller such as PID, MPC, and others during computer simulations.

Two key contribution steps of this research/paper stand out: The first step is: Test the vehicle model with 4-wheel drive in the computational form [16-17], this being the objective of the work. The second step (for later work): Validate it on a platform/simulator (Hardware in the Loop). However, these modeling steps (testing and validation) are necessary for the vehicle system to achieve optimum performance and handling safety, in addition to reducing implementation costs [18-19].

The mathematical model (represented in a computational way through the Simulink® application) respectively, its blocks provide inputs and outputs that determine the vehicle system as a whole [20-21], as shown in Fig. 1.

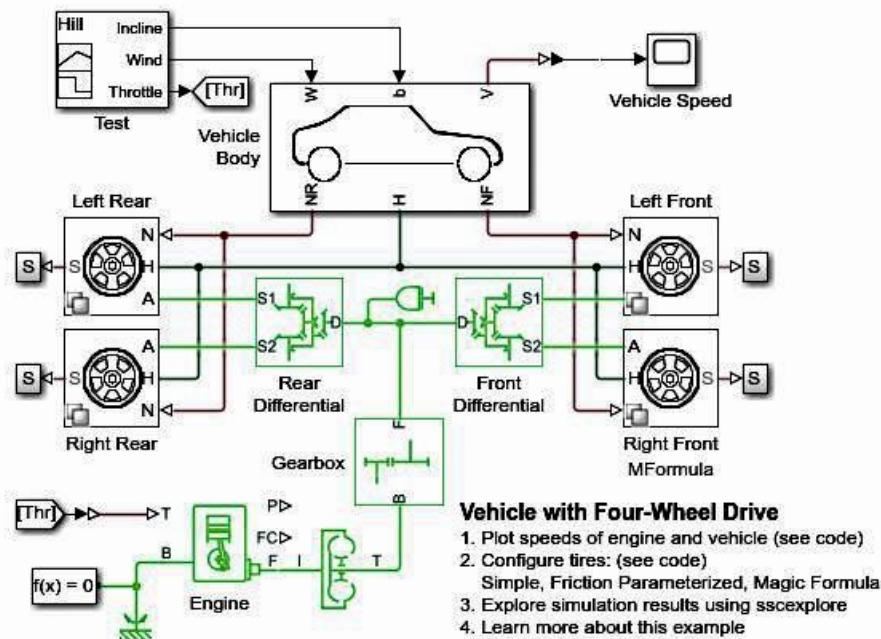
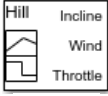
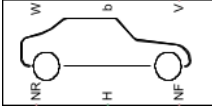
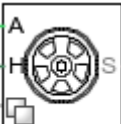
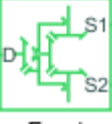


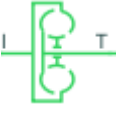
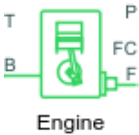
Fig. 1. A computational model of the vehicle with 4-wheel drive

Each block used in the model of the vehicle (Fig. 1) is described in Table 1. The configuration or modeling of the vehicle system blocks was developed through the software Matlab®/Simulink® [23] to present computational simulations closer to reality [24-25].

This proposed paper has the following structure: 1. Introduction; 2. Mathematical Model of the Vehicle with Traction in 4-Wheels; 3. Calibrations Parameters; 4. Additional Parameters to Calibrating the 4-Wheel Vehicle; 5. Results; 6. Final Considerations.

**Table 1.** Description and illustration of the blocks used in vehicle modeling

Component	Name	Descriptions
	Signal builder	Create and generate interchangeable groups of signals whose waveforms are piecewise linear.
	Go to	Send signals from blocks that have the specified tag.
	Vehicle body	Represents a two-axle vehicle body in longitudinal movement. The block accounts for body mass, aerodynamic drag, road incline, and weight distribution between axles due to acceleration and road profile.
	Constant	Output the constant specified by the constant value parameter if a constant value is a vector and interpret vector parameters as 1-D is on, treat the constant values as a 1-D array.
	Tire (Magic formula)	Constant of slip, assigned to each tire respectively. Represents the longitudinal behavior of a highway tire. The block is built from Tire-Road Interaction (Magic Formula) and Simscape™ Foundation Library Wheel and Axle blocks. Optionally, the effects of tire inertia, stiffness, and damping can be included.
	Tire (Magic formula)	Represents the longitudinal behavior of a highway tire. The block is built from Tire-Road Interaction (Magic Formula) and Simscape™ Foundation Library Wheel and Axle blocks. Optionally, the effects of tire inertia, stiffness, and damping can be included.
	Tire (Magic formula)	Represents the longitudinal behavior of a highway tire. The block is built from Tire-Road Interaction (Magic Formula) and Simscape™ Foundation Library Wheel and Axle blocks. Optionally, the effects of tire inertia, stiffness, and damping can be included.
	Tire (Magic formula)	Represents the longitudinal behavior of a highway tire. The block is built from Tire-Road Interaction (Magic Formula) and Simscape™ Foundation Library Wheel and Axle blocks. Optionally, the effects of tire inertia, stiffness, and damping can be included.
	Scope	Displays input signals with respect to simulation time.
	Vehicle Speed	
	Rear Differential	This block represents a differential arranged like a planetary bevel gear train equipped with an additional bevel gear transmission between the transmission shaft and the support. The pinion gear of this transmission is attached to the transmission shaft, while the large bevel gear is attached to the support. No conformity is modeled on this block. It can optionally include inertia and losses due to gear gears and viscous friction of the bearing.
	Front Differential	This block represents a differential arranged like a planetary bevel gear train equipped with an additional bevel gear transmission between the transmission shaft and the support. The pinion gear of this transmission is attached to the transmission shaft, while the large bevel gear is attached to the support. No conformity is modeled on this block. It can optionally include inertia and losses due to gear gears and viscous friction of the bearing.
	Driveshaft Inertia	The block represents an ideal rotational mechanical inertia. It has a mechanical rotational conservation door. The block's positive direction from its door to the reference point is considered. This means that the inertia torque is positive if the inertia is accelerated in the positive direction.

	<b>Gearbox/Simple Gear</b>	This block represents a fixed-ratio gear or gearbox. No inertia or compliance is modeled on this block. It can optionally include gears and viscous bearing losses.
	<b>Torque Converter</b>	This block represents a three-part torque converter that has an impeller, turbine, and stator. The model is only valid for positive impeller speeds but supports the simulation of driving modes (energy flowing from the impeller to the turbine) and inertia (energy flowing from the turbine to the impeller).
	<b>Engine/Generic Engine</b>	This block represents a system-level model of spark ignition and diesel engines specified for use at initial modeling levels when only basic parameters are available. Optional idle and red line controllers are included.
	<b>Mechanical Rotational Reference From</b>	This block represents a given mechanical rotation reference point (a frame or a floor). Use it to connect mechanical rotational doors that are rigidly attached to the structure (ground). Receives signals from the Go to block with the specified tag.
	<b>Solver Configuration</b>	Defines the solver settings to use in the simulation.

## 2. Mathematical Model of the Vehicle with Traction in 4-Wheels

For the mathematical model of the vehicle with 4-wheel drive [26, 27], the dynamics and movement [28] parameters of the vehicle are considered, with the restriction or limitation that the vehicle does not move vertically in relation to the ground [29], as shown in Fig. 2. The main variables presented in Fig. 2 are described in Table 2.

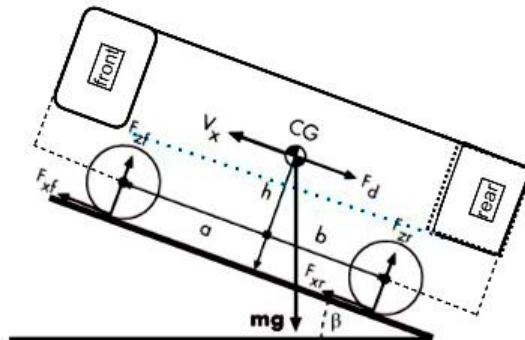


Fig. 2. Wheel drive vehicle dynamics and movement

Table 2. Main variables of the mathematical model

Variables	Descriptions
$g$	Gravitational acceleration
$\beta$	Incline angle
$m$	Mass of the vehicle
$h$	Vehicle center of gravity (CG) height above ground
$a, b$	Distance between the front and rear axles, respectively, from the normal projection point of the vehicle's CG on the plane of the common axis
$V_x$	Vehicle speed. When $V_x > 0$ the vehicle moves forward. When $V_x < 0$ , the vehicle moves backward.
$V_w$	Wind speed. When $V_w > 0$ , the wind is the opposite. When $V_x < 0$ , the wind is tail.
$n$	Number of wheels on each axle
$F_{xf}, F_{xr}$	Longitudinal forces on each wheel at the front and rear ground contact points, respectively
$F_{zf}, F_{zr}$	Normal load forces on each wheel at the front and rear ground contact points, respectively
$A$	The effective front cross-sectional area of the vehicle
$C_d$	Aerodynamic drag coefficient
$\rho$	The mass density of air
$F_d$	Aerodynamic drag force

The longitudinal forces [30, 31] of the tire move the vehicle backward or forwards. The movement of the vehicle is the result of the sum of all the forces and torques that act on the vehicle [32-34]. The vehicle's center of gravity (CG) allows the weight mass gravity ( $mg$ ) to be active, depending on the angle of inclination ( $\beta$ ) the weight has the ability to pull the vehicle to the ground, as well as to pull back or forward [35, 36]. The aerodynamic resistance slows the vehicle in terms of movement [37, 38], regardless of whether it moves backward or forwards. In [39], it is determined that the aerodynamic drag force ( $F_d$ ) acts on the center of gravity (CG) starting from the second law of Isaac Newton, according to Equation 1.

$$m\dot{V}_x = F_x - F_d - mg \sin \beta \quad (1)$$

where ( $V_x$ ) indicates the acceleration in relation to the axis (x), that is, the dynamics of the speed and ( $F_x$ ) is the longitudinal force of the axis (x), which can be calculated [39-41] according to Equation 2.

$$F_x = n(F_{xf} + F_{xr}) \quad (2)$$

The aerodynamic drag force ( $F_d$ ) is calculated [42, 43] using Equation 3.

$$F_d = \frac{1}{2} C_{d\rho} A (V_x + V_w)^2 \operatorname{sgn}(V_x + V_w) \quad (3)$$

Zero pitch torque and normal zero acceleration determine the normal forces for each wheel, respectively. The normal force ( $F_{zf}$ ) on each front wheel [44, 45] is described by the following Equation 4.

$$F_{zf} = \frac{-h(F_d + mg \sin \beta + m\dot{V}_x) + b mg \cos \beta}{n(a + b)} \quad (4)$$

The normal force ( $F_{zr}$ ) on each rear wheel [45] is described by Equation 5.

$$F_{zr} = \frac{h(F_d + mg \sin \beta + m\dot{V}_x) + a mg \cos \beta}{n(a + b)} \quad (5)$$

However, the sum of normal forces [45, 46] is calculated using Equation 6.

$$F_{zf} + F_{zr} = mg \frac{\cos \beta}{n} \quad (6)$$

In [46-49], the throwing dynamics originate from the inclination rate ( $\alpha$ ) that occurs during the acceleration of the vehicle depending on three torque elements and the vehicle's inertia, according to Equation 7.

$$\alpha = \frac{(f h) + (F_{zf} a) - (F_{zr} b)}{j} \quad (7)$$

Being ( $a$ ) the pitch rate; ( $f$ ) longitudinal force; and ( $j$ ) inertia, this mathematical modeling is inserted into the vehicle body block, allowing only the longitudinal dynamics to be modeled, oriented during the direction of movement parallel to the ground [50, 51]. The vehicle is guaranteed to be in normal and inclined balance. Through Simscape™ (application of the Simulink® environment) [52, 53], it is possible to explore and manipulate the variables of each block as well as the generation of their figures, from the input of physical signals to the output of physical signals from the vehicle system as a whole. The vehicle body block does not model lateral movement, and the equations ensure that the wheels do not lose contact with the ground.

### 3. Calibrations Parameters

The physical input signals (signal builder) are valid only for the movement or longitudinal position of the vehicle body [54, 55], considering that the steering wheel of the vehicle remains straight (parallel to the road) for the set of vehicle pedals, the acceleration is determined as the input only [56]. In addition, the minimum longitudinal force ( $F_x$ ) required to brake the vehicle, can be calculated from Equation 1.

The major three physical input signals (slope, wind, accelerator) [57] are defined with the following values proposed in Table 3. Fig. 3 shows the graphs corresponding to the input signals described in Table 3.

**Table 3.** Input signal parameters and descriptions

Descriptions	Values	Units
Incline	15	(°)
Wind	0	$m/s$
Throttle	0.4	$m/s^2$

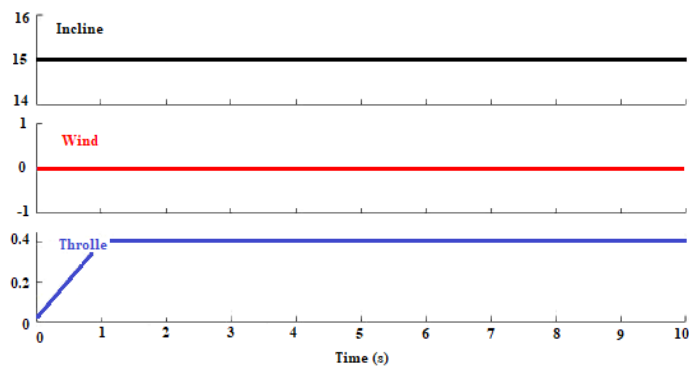


**Fig. 3.** Physical input signals of the three parameters considered

#### 3.1. Vehicle Body

The vehicle body subsystem [58] presents a diagram with its main variables and task assignments, as shown in Fig. 4. The variables that make up the vehicle body subsystem diagram are detailed in Table 4. Some variables of vehicle body subsystems can be added or simplified to meet the desired design [58-59].

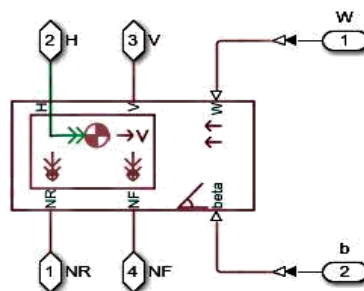


**Fig. 4.** Vehicle body subsystem

**Table 4.** Variables of vehicle body subsystem

Variables	Descriptions	Units
H	Mechanical translational conservation door linked to the horizontal movement of the vehicle body	$m$
V	Vehicle speed	$m/s$
NR	Normal rear-wheel forces	$N$
NF	Normal front wheel forces	$N$
w	Headwind speed	$m/s$
b	Inclination angle	(°)

#### 4. Additional Parameters to Calibrating the 4-Wheel Vehicle

For the calibration of the 4-wheel vehicle, it was determined some variables that support a real-time simulation [59] are not far from reality, as described in Table 5. After the calibration parameters are added, the system response (results) is represented in graphical form.

**Table 5.** Additional parameters for vehicle calibration [59, 60]

Descriptions	Values	Units
Beta (b)	15	(°)
Engine rotation	800	RPM
Driveshaft inertia	12	Kgm <sup>2</sup>
Lateral inertia	4.1290	Kgm <sup>2</sup>
Mass of the vehicle	1500	Kg
Wheel radius	0.4046	m
Tire damping	1000	N/(m/s)
Tire stiffness	200000	N/m
Ratio differential constant	2	--

#### 5. Results and Discussion

After considering the values in Table 3 and Table 5, respectively, the three physical output signals of the system are shown, highlighted as car speed, engine speed, and acceleration [60], according to Fig. 5.

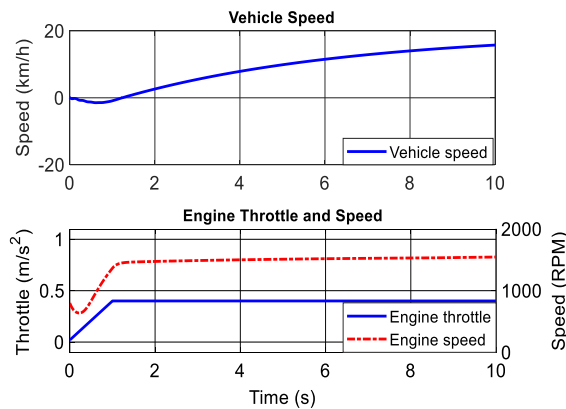


**Fig. 5.** Physical output signals of the three parameters considered (1)

The outputs of the physical signals from the vehicle system can also be considered the normal force of the front wheels (NF) and the normal force of the rear wheels (NR), as shown in Fig. 6, respectively.

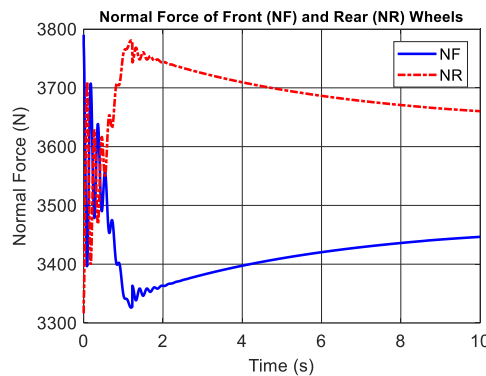


**Fig. 6.** Normal forces NF and NR, respectively (1)

Normal forces are valid when the vehicle's wheel comes into contact with the ground, i.e., when the total weight of the vehicle is considered during longitudinal movement.

### 5.1. Change in Calibration Values

For the second simulation, it is necessary to change the values of engine speed, vehicle mass, and wheel radius (the radius of the wheels is unchanged, as well as the other items in Table 5). As described in Table 6, the physical input signals remain unchanged. Fig. 7 shows the graphical behavior of the output of the three physical signals.

**Table 6.** Change in calibration values [13, 31]

Descriptions	Values	Units
Engine rotation	2500	RPM
Mass of the vehicle	1800	Kg
Wheel radius	0.4046	m

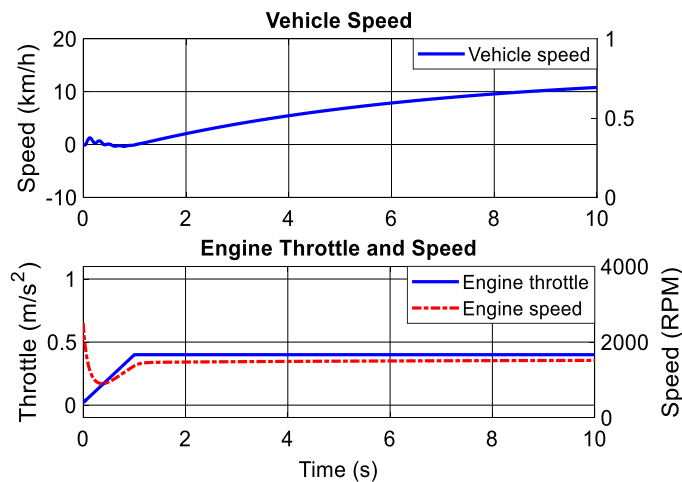


**Fig. 7.** The three output signals from the second calibration (2)

The outputs of the physical signals from the vehicle system can also be considered the normal force of the front wheels (NF) and the normal force of the rear wheels (NR) are shown in Fig. 8, respectively. Normal forces are valid when the vehicle's wheel comes into contact with the ground, i.e., when the total weight of the vehicle is considered during longitudinal movement.

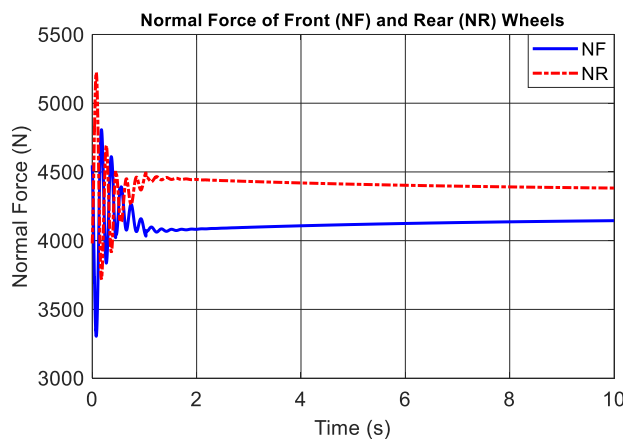


**Fig. 8.** Normal forces NF and NR, respectively (2)

Fig. 3 shows the three physical input signals for modeling the vehicle with a 4-wheel drive. The dynamics of the 4 tires were determined as a magic formula type. Table 3 shows the primary calibration parameters considering as complete some additional parameters for the vehicle calibration proposed in Table 5. As a result, 3 output signals are generated (vehicle speed, angular speed, and the

engine accelerator), as shown in Fig. 5. It is shown in Table 6 altered data from the second calibration for comparison purposes, which generates Fig. 7 consisting of the three physical output signals (vehicle speed, angular speed, and the engine accelerator).

Note that in the first calibration (results in Fig. 5), considering the vehicle at a ( $15^\circ$ ) inclination (from front to rear position), the vehicle rolls (descends) with an approximate speed of ( $16 \text{ km/h}$ ). The angular speed of the engine is 1550 RPM which quickly manages to attend the intervention of the opposite movement of the vehicle rolling, that is, after operating the pedal with an acceleration of ( $0.4 \text{ m/s}^2$ ) it produces an angular speed of the engine that covers the transmission and differential to the tires, which allows the vehicle to move longitudinally, and the normal force of the vehicle is greater than the opposite force, the output of the angular speed is above the exit or entry of the accelerator.

In the second calibration (values in Table 6) of the vehicle (results in Fig. 7), considering the vehicle at an inclination of  $15^\circ$  (from front to rear position), the vehicle rolls (descends) with an approximate speed of ( $11 \text{ km/h}$ ). The angular speed of the engine is 1500 RPM and cannot prevent or overcome the opposite movement of the vehicle rolling, that is, after operating the pedal with an acceleration of ( $0.4 \text{ m/s}^2$ ) it produces an angular speed of the engine that covers the transmission and differential up to the tires, which allows the vehicle to move longitudinally, and the normal force of the vehicle is less than the opposite force, the angular speed output is below the accelerator exit or entry.

The Matlab<sup>®</sup>/Simulink<sup>®</sup> software consists of a library described as a Simulink<sup>™</sup> library browser where the blocks in Table 1 can be explored in detail and provide enough information to calibrate the desired system. For the generation of graphs or figures of each block in the modeling of the vehicle with a 4-wheel drive, the integrated library described as Simscape<sup>™</sup> results explorer (Fig. 1) is responsible for generating each one in detail.

In Fig. 6, the normal forces of the front and rear wheels are illustrated, respectively, considering the primary calibration values of Table 3 and Table 5 (additional parameters). In Fig. 8, the normal forces of the front and rear wheels are illustrated, respectively, considering the secondary calibration values in Table 6 and Table 5 (some additional parameters). Fig. 6 shows a lower result compared to Fig. 8. This is due to the fact that the rotation of the vehicle's engine is less than the mass of the vehicle, leading the vehicle system to a longer response time or recognition of the wheels on the ground. The result of Fig. 8 is the opposite. The vehicle's engine rotation exceeds the vehicle's mass, which results in quick recognition of the vehicle's wheels on the ground.

Unlike the results presented in the articles [7, 13, 18, 20, 29, 32, 41, 42, 51], this paper presents a sequence of results during the analysis of the internal combustion engine performance, normal front and rear wheel forces with comparative changes of real vehicle parameters (in particular engine speed and vehicle mass), the longitudinal control modeling of the 4-wheeled vehicle presented excellent results represented by the physical output signals; vehicle speed, engine speed, and acceleration.

Simscape<sup>™</sup> (application of the Simulink<sup>®</sup> environment) is used to develop control systems and test the performance of the system, in addition to obtaining a range of resources that can be used according to the purpose of the project, supports the generation of C code for the implementation of models in different simulation environments (SIL or HIL).

## 6. Conclusions

According to the results of the computational simulations, when considering a slope in the vehicular system to perform parallel, perpendicular, and oblique parking maneuvers during front or rear displacement, a maximum engine angular speed of ( $800 \text{ RPM}$ ) is recommended because it is a generic engine (internal combustion), higher values extrapolate the longitudinal validation for this proposed calibration model, the adjustments depend on the project application/implementation and can be calibrated with different physical parameters of the input signal. If needed, changing the type of tire dynamics can help to get better results.

As contributions, the results of this paper guarantee: I. Adequate performance of the operational vehicle system with internal combustion engine associated with some real calibration parameters; II. Even when the vehicle is in an angular inclined position during the automatic parking maneuvers; III. The engine angular speed range (800 RPM) determines the solid validation of the computational modeling (Software in the Loop); IV. Time and electronic components savings; V. Further validation (Hardware in the Loop).

For future research, it is considered to increase the speed during vehicle maneuvers and adapt the longitudinal modeling to suit robust systems such as Four-wheel-drive (4WD) or Front-wheel-drive (FWD) vehicles with speeds greater than 30 km/h during highway travel, establish an operating range greater than 800 RPM relative to the angular speed of the engine, including adverse conditions such as obstacles, noise, or disturbances in the vehicle system, and show the best results during computer simulations and subsequent HIL-Hardware in-the Loop validation.

**Author Contribution:** All authors contributed equally to the main contributor to this paper. All authors read and approved the final paper.

**Acknowledgment:** The authors acknowledge the CAPES, FAPESP, and CNPq, both Brazilian research funding agencies. The fourth author thanks CNPq for the financial support (Process: 310562/2021-0).

**Conflicts of Interest:** The authors declare no conflict of interest.

## References

- [1] R. Anbazhagan, B. Satheesh, and K. Gopalakrishnan, "Mathematical modeling and simulation of modern cars in the role of stability analysis," *Indian Journal of Science and Technology*, vol. 6, no. 5, pp. 4633-4641, 2013, <http://dx.doi.org/10.17485/ijst/2013/v6isp5.9>.
- [2] H. P. Oliveira, A. J. Sousa, A. P. Moreira, P. J. Costa, and A. D. Rodi, "Modeling and assessing of omnidirectional robots with three and four wheels," *Contemporary Robotics: Challenges and Solutions*, pp. 109-138, 2009, <http://dx.doi.org/10.5772/7796>.
- [3] Y. J. Chen, Q. S. Lei, X. Zhang, G. H. Zheng, and Y. F. Zhang, "Suspension System Dynamics Modeling and Simulation Analysis," *DEStech Transactions on Engineering and Technology Research (icamm)*, 2017, <http://dx.doi.org/10.12783/dtetr/icamm2016/7397>.
- [4] J. Kong, M. Pfeiffer, G. Schildbach, and F. Borrelli, "Kinematic and dynamic vehicle models for autonomous driving control design," *IEEE Intelligent Vehicles Symposium (IV)*, pp. 1094-1099, 2015, <https://doi.org/10.1109/IVS.2015.7225830>.
- [5] A. Elhefnawy, H. Ragheb, A. M. Sharaf, and S. Hegazy, "On the control strategies for vehicle stability enhancement," *International Journal of Heavy Vehicle Systems*, vol. 27, no. 5, pp. 622-647, 2020, <https://doi.org/10.1504/IJHVS.2020.111263>.
- [6] H. Haiyan, and H. Qiang, "Three-dimensional modeling and dynamic analysis of four-wheel-steering vehicles," *Acta Mechanica Sinica*, vol. 19, no. 1, pp. 79-88, 2003, <https://doi.org/10.1007/BF02487456>.
- [7] A. Chebly, R. Talj, and A. Charara, "Coupled longitudinal and lateral control for an autonomous vehicle dynamics modeled using a robotics formalism," *IFAC-PapersOnLine*, vol. 50, no. 1, pp. 12526-12532, 2017, <https://doi.org/10.1016/j.ifacol.2017.08.2190>.
- [8] Z. Alqarni, "Improved Control Strategy for 4 WD Electric Vehicle Using Direct Torque Control Technique with Space Vector Modulation," *2022 IEEE 12th Annual Computing and Communication Workshop and Conference (CCWC)*, pp. 0816-0822, 2022, <https://doi.org/10.1109/CCWC54503.2022.9720858>.
- [9] P. Wrzeczniarz, W. Ambroszko, and A. Pindel, "Limitations of vehicle movement resistances: aerodynamic resistance," *AUTOBUSY-Technika, Eksploatacja, Systemy Transportowe*, vol. 19, no. 12, pp. 252-255, 2018, <https://doi.org/10.24136/atest.2018.393>.

- 
- [10] T. H. Hsu, J. F. Liu, P. N. Yu, W. S. Lee, and J. S. Hsu, "Development of an automatic parking system for vehicle," *IEEE Vehicle Power and Propulsion Conference*, pp. 1-6, 2008, <https://doi.org/10.1109/VPPC.2008.4677655>.
- [11] A. Gupta, R. Divekar, and M. Agrawal, "Autonomous parallel parking system for Ackerman steering four wheelers," *IEEE International Conference on Computational Intelligence and Computing Research*, pp. 1-6, 2010, <https://doi.org/10.1109/ICCIC.2010.5705869>.
- [12] C. J. T. Manuel, "Design and development of algorithms and control strategies for automatic parking systems: advanced driver assistance system," *Master's thesis, Universidade Tecnológica Federal do Paraná*, 2020, <http://repositorio.utfpr.edu.br/jspui/handle/1/24096>.
- [13] J. Huang, Y. Chen, X. Peng, L. Hu, and D. Cao, "Study on the driving style adaptive vehicle longitudinal control strategy," *IEEE/CAA Journal of Automatica Sinica*, vol. 7, no. 4, pp. 1107-1115, 2020, <https://doi.org/10.1109/JAS.2020.1003261>.
- [14] T. Chen, H. Huang, Q. Li, Z. Mo, Z. Feng, and J. Huang, "Drive Control Strategy Design for FSEC Racing Car," *Proceedings of China SAE Congress 2020: Selected Papers*. Springer, Singapore, pp. 255-276, 2022, [https://doi.org/10.1007/978-981-16-2090-4\\_15](https://doi.org/10.1007/978-981-16-2090-4_15).
- [15] J. Antunes, A. Antunes, P. Outeiro, C. Cardeira, and P. Oliveira, "Testing of a torque vectoring controller for a Formula Student prototype," *Robotics and Autonomous Systems*, vol. 113, pp. 56-62, 2019, <https://doi.org/10.1016/j.robot.2018.12.010>.
- [16] A. Buyval, A. Gabdullin, A. Klimchik, "Model Predictive Path Integral Control for Car Driving with Dynamic Cost Map," *Proceedings of the 15th International Conference on Informatics in Control, Automation and Robotics*, vol. 1, pp. 248-254, 2018, <https://doi.org/10.5220/0006901702480254>.
- [17] B. M. Notaroš, R. McCullough, S. B. Manić, and A. A. Maciejewski, "Computer-assisted learning of electromagnetics through MATLAB programming of electromagnetic fields in the creativity thread of an integrated approach to electrical engineering education," *Computer Applications in Engineering Education*, v. 27, n. 2, p. 271-287, 2019, <https://doi.org/10.1002/cae.22073>.
- [18] R. Attia, R. Orjuela, and M. Basset, "Combined longitudinal and lateral control for automated vehicle guidance," *Vehicle System Dynamics*, vol. 52, no. 2, pp. 261-279, 2014, <https://doi.org/10.1080/00423114.2013.874563>.
- [19] Y. Chen, S. Chen, T. Zhang, S. Zhang, and N. Zheng, "Autonomous vehicle testing and validation platform: Integrated simulation system with hardware in the loop," *2018 IEEE Intelligent Vehicles Symposium (IV)*, pp. 949-956, 2018, <https://doi.org/10.1109/IVS.2018.8500461>.
- [20] B. M. Nguyen, H. V. Nguyen, M. Ta-Cao, and M. Kawanishi, "Longitudinal Modelling and Control of In-Wheel-Motor Electric Vehicles as Multi-Agent Systems," *Energies*, vol. 13, no. 20, pp. 5437, 2020, <https://doi.org/10.3390/en13205437>.
- [21] G. Rill and A. A. Castro, "Road Vehicle Dynamics: Fundamentals and Modeling with MATLAB® (2nd ed)," *CRC Press*, 2020, <https://doi.org/10.1201/9780429244476>.
- [22] Mathworks, "Vehicle with four-wheel drive, 2020, <https://www.mathworks.com/help/physmod/sdl/ug/vehicle-with-four-wheel-drive.html>.
- [23] A. Szántó, and G. A. Sziki, "Review of Modern Vehicle Powertrains and Their Modelling and Simulation in MATLAB/Simulink," *International Journal of Engineering and Management Sciences*, vol. 5, no. 2, pp. 232-250, 2020, <https://doi.org/10.21791/IJEMS.2020.2.29>.
- [24] J. Tarnawski, and T. Karla, "Real-time simulation in non real-time environment," *21st International Conference on Methods and Models in Automation and Robotics (MMAR)*, pp. 577-582, 2016, <https://doi.org/10.1109/MMAR.2016.7575200>.
- [25] S. Lekshmi, and P. S. Lal Priya, "Mathematical modeling of Electric vehicles-A survey," *Control Engineering Practice*, vol. 92, pp. 104138, 2019, <https://doi.org/10.1016/j.conengprac.2019.104138>.
- [26] S. Sundar, T. Sudarsanan, and R. Krishnan, "Review of Design and Fabrication of four wheel Steering system," *International Journal of Recent Trends in Engineering and Research (IJRTER)*, vol. 4, no. 10, pp. 1034-1049, 2018, <https://doi.org/10.23883/IJRTER.2018.4386.3THDB>.
-

- [27] C. Habermehl, G. Jacobs, and S. Neumann, "A modeling method for gear transmission efficiency in transient operating conditions," *Mechanism and Machine Theory*, vol. 153, pp. 103996, 2020, <https://doi.org/10.1016/j.mechmachtheory.2020.103996>.
- [28] H. Dugoff, P. S. Fancher, and L. Segel, "An analysis of tire traction properties and their influence on vehicle dynamic performance," *SAE transactions*, vol. 79, pp. 1219-1243, 1970, <https://doi.org/10.4271/700377>.
- [29] T. Chen, X. Xu, L. Chen, H. Jiang, Y. Cai, and Y. Li, "Estimation of longitudinal force, lateral vehicle speed and yaw rate for four-wheel independent driven electric vehicles," *Mechanical Systems and Signal Processing*, vol. 101, pp. 377-388, 2018, <https://doi.org/10.1016/j.ymsp.2017.08.041>.
- [30] S. Yang, Y. Lu, and S. Li, "An overview on vehicle dynamics," *International Journal of Dynamics and Control*, vol. 1, no. 4, pp. 385-395, 2013, <https://doi.org/10.1007/s40435-013-0032-y>.
- [31] M. Viehweger, C. Vasseur, S. van Aalst, M. Acosta, E. Regolin, A. Alatorre, W. Desmet, F. Naets, V. Ivanov, A. Ferrara, and A. Victorino, "Vehicle state and tyre force estimation: demonstrations and guidelines," *Vehicle system dynamics*, vol. 59, no. 5, pp. 675-702, 2021, <https://doi.org/10.1080/00423114.2020.1714672>.
- [32] J. Zhang, Y. Yang, M. Hu, Z. Yang, and C. Fu, "Longitudinal-Vertical Comprehensive Control for Four-Wheel Drive Pure Electric Vehicle Considering Energy Recovery and Ride Comfort," *Energy*, vol. 236, pp. 121417, 2021, <https://doi.org/10.1016/j.energy.2021.121417>.
- [33] J. Woo, J. Park, C. Yu, and N. Kim, "Dynamic model identification of unmanned surface vehicles using deep learning network," *Applied Ocean Research*, vol. 78, pp. 123-133, 2018, <https://doi.org/10.1016/j.apor.2018.06.011>.
- [34] A. O. Kiyakli, and H. Solmaz, "Modeling of an electric vehicle with MATLAB/Simulink," *International Journal of automotive science and technology*, vol. 2, no. 4, pp. 9-15, 2018, <https://doi.org/10.30939/ijastech.475477>.
- [35] D. W. Karmiadji, M. Gozali, M. Setiyo, T. Raja, and T. A. Purnomo, "Comprehensive Analysis of Minibuses Gravity Center: A Post-Production Review for Car Body Industry," *Mechanical Engineering for Society and Industry*, vol. 1, no. 1, pp. 31-40, 2021, <https://doi.org/10.31603/mesi.5250>.
- [36] G. Park, and S. B. Choi, "An Integrated Observer for Real-Time Estimation of Vehicle Center of Gravity Height," *IEEE Transactions on Intelligent Transportation Systems*, vol. 22, no. 9, pp. 5660-5671, 2020, <https://doi.org/10.1109/TITS.2020.2988508>.
- [37] J. R. Piechna, K. Kurec, J. Broniszewski, M. Remer, A. Piechna, K. Kamieniecki, K. and P. Bibik, "Influence of the Car Movable Aerodynamic Elements on Fast Road Car Cornering," *Energies*, vol. 15, no. 3, pp. 689, 2022, <https://doi.org/10.3390/en15030689>.
- [38] F. J. Morales, and F. G. Benitez, "Considerations on the operation of inertial continuous variable transmissions," *Mechanism and Machine Theory*, vol. 144, pp. 103672, 2020, <https://doi.org/10.1016/j.mechmachtheory.2019.103672>.
- [39] T. D. Gillespie, "Fundamentals of vehicle dynamics," *SAE Technical Paper*, vol. 114, 1992, <https://www.sae.org/publications/technical-papers/content/R-114/>.
- [40] Q. Wu, Y. Sun, M. Spiriyagin, and C. Cole, "Railway track longitudinal force model," *Vehicle System Dynamics*, vol. 59, no. 1, pp. 155-170, 2021, <https://doi.org/10.1080/00423114.2019.1673445>.
- [41] İ. C. Güteryüz, and Ö. Başer, "Modelling the longitudinal braking dynamics for heavy-duty vehicles," *Proceedings of the Institution of Mechanical Engineers, Part D: Journal of Automobile Engineering*, vol. 235, no. (10-11), pp. 2802-2817, 2021, <https://doi.org/10.1177/09544070211004508>.
- [42] P. Shakouri, A. Ordys, M. Askari, and D. S. Laila, "Longitudinal vehicle dynamics using Simulink/Matlab," *UKACC International Conference on Control*, pp. 1-6, 2010, <https://doi.org/10.1049/ic.2010.0410>.
- [43] M. P. Bauskar, D. Y. Dhande, S. Vadgeri, and S. R. Patil, "Study of aerodynamic drag of sports utility vehicle by experimental and numerical method," *Materials Today: Proceedings*, vol. 16, pp. 750-757, 2019, <https://doi.org/10.1016/j.matpr.2019.05.155>.

- 
- [44] M. Amodeo, A. Ferrara, R. Terzaghi, and C. Vecchio, "Wheel slip control via second-order sliding-mode generation," *IEEE Transactions on Intelligent Transportation Systems*, vol. 11, no. 1, pp. 122-131, 2009, <https://doi.org/10.1109/TITS.2009.2035438>.
- [45] U. Kiencke, "Realtime estimation of adhesion characteristic between tyres and road," *IFAC Proceedings*, vol. 26, no. 2, pp. 15-18, 1993, [https://doi.org/10.1016/S1474-6670\(17\)48673-3](https://doi.org/10.1016/S1474-6670(17)48673-3).
- [46] A. Genovese, and F. Timpone, "Tyre Mechanics and Thermal Effects on Tyre Behaviour," *B. Lenzo (eds) Vehicle Dynamics, CISM International Centre for Mechanical Sciences*, Springer, Cham, vol. 603, pp. 139-192, 2022, [https://doi.org/10.1007/978-3-030-75884-4\\_3](https://doi.org/10.1007/978-3-030-75884-4_3).
- [47] C. Liu, J. Zhou, A. Gerhard, J. Kubenz, and G. Prokop, "Characterization of the Vehicle Roll Movement with the Dynamic Chassis Simulator," *Vehicle and Automotive Engineering*. Springer, Cham, pp. 129-141, 2018, [https://doi.org/10.1007/978-3-319-75677-6\\_11](https://doi.org/10.1007/978-3-319-75677-6_11).
- [48] B. M. Nguyen, S. Hara, H. Fujimoto, and Y. Hori, "Slip control for IWM vehicles based on hierarchical LQR," *Control Engineering Practice*, vol. 93, pp. 104179, 2019, <https://doi.org/10.1016/j.conengprac.2019.104179>.
- [49] K. El Majdoub, F. Giri, H. Ouadi, L. Dugard, and F. Z. Chaoui, "Vehicle longitudinal motion modeling for nonlinear control," *Control Engineering Practice*, vol. 20, no. 1, pp. 69-81, 2012, <https://doi.org/10.1016/j.conengprac.2011.09.005>.
- [50] E. Esmailzadeh, G. R. Vossoughi, and A. Goodarzi, "Dynamic modeling and analysis of a four motorized wheels electric vehicle," *Vehicle System Dynamics*, vol. 35, no. 3, pp. 163-194, 2001, <https://doi.org/10.1076/vesd.35.3.163.2047>.
- [51] H. Zhou, F. Jia, H. Jing, Z. Liu, and L. Güvenç, "Coordinated longitudinal and lateral motion control for four wheel independent motor-drive electric vehicle," *IEEE transactions on Vehicular Technology*, vol. 67, no. 5, pp. 3782-3790, 2018, <https://doi.org/10.1109/TVT.2018.2816936>.
- [52] K. Miura, S. Tokunaga, N. Ota, Y. Tange, and T. Azumi, "Autoware toolbox: Matlab/simulink benchmark suite for ROS-based self-driving software platform," *Proceedings of the 30th International Workshop on Rapid System Prototyping (RSP'19)*, pp. 8-14, 2019, <https://doi.org/10.1145/3339985.3358494>.
- [53] N. Deo, A. Rangesh and M. M. Trivedi, "How would surround vehicles move? a unified framework for maneuver classification and motion prediction," *IEEE Transactions on Intelligent Vehicles*, vol. 3, no. 2, pp. 129-140, 2018, <https://doi.org/10.1109/TIV.2018.2804159>.
- [54] Z. Zhang, C. Wang, W. Zhao, and J. Feng, "Longitudinal and lateral collision avoidance control strategy for intelligent vehicles," *Proceedings of the Institution of Mechanical Engineers, Part D: Journal of Automobile Engineering*, vol. 236, no. (2-3) pp. 268-286, 2022, <https://doi.org/10.1177/09544070211024048>.
- [55] T. Yang, Z. Bai, Z. Li, N. Feng, and L. Chen, "Intelligent Vehicle Lateral Control Method Based on Feedforward + Predictive LQR Algorithm," *Actuators*, vol. 10, no. 9, p. 228, Sep. 2021, <http://dx.doi.org/10.3390/act10090228>.
- [56] D. Schramm, M. Hiller, and R. Bardini, "Vehicle Dynamics: Modeling and Simulation," *Springer*, Berlin, Heidelberg, 2018, <https://doi.org/10.1007/978-3-662-54483-9>.
- [57] M. Tomasikova, D. Sojcak, A. Nieoczym, and F. Brumercik, "Experimental data in vehicle modeling," *LOGI-Scientific Journal on Transport and Logistics*, vol. 8, no. 1, pp. 82-87, 2017, <https://doi.org/10.1515/logi-2017-0010>.
- [58] M. Yue, X. Wei, and Z. Li Z, "Adaptive sliding-mode control for two-wheeled inverted pendulum vehicle based on zero-dynamics theory," *Nonlinear Dynamics*, vol. 76, no 1, pp. 459-471, 2014, <https://doi.org/10.1007/s11071-013-1139-6>.
- [59] Renault Captur, "Manual of proprietary," 2020, <https://www.renault.com.br/manuais/captur.html>.
- [60] C. J. T. Manuel, M. M. D. Santos, A. M. Tusset, "Mathematical modeling attributed to kinematics and dynamics of a vehicle with 4-wheels," *The European Physical Journal Special Topics*, vol. 230, no. 18, pp. 3663-3672, 2021, <https://doi.org/10.1140/epjs/s11734-021-00238-2>.
-